Liouvillian Skin Effect: Slowing Down of Relaxation Processes without Gap Closing

Taiki Haga,[1,2,*] Masaya Nakagawa,[2] Ryusuke Hamazaki,[2,3] and Masahito Ueda[2,4,5]
[1]Department of Physics and Electronics, Osaka Prefecture University, Sakai-shi, Osaka 599-8531, Japan
[2]Department of Physics, University of Tokyo, 7-3-1 Hongo, Bunkyo-ku, Tokyo 113-0033, Japan
[3]Nonequilibrium Quantum Statistical Mechanics RIKEN Hakubi Research Team, RIKEN Cluster for Pioneering Research (CPR), RIKEN iTHEMS, Wako, Saitama 351-0198, Japan
[4]RIKEN Center for Emergent Matter Science (CEMS), Wako, Saitama 351-0198, Japan
[5]Institute for Physics of Intelligence, University of Tokyo, 7-3-1 Hongo, Bunkyo-ku, Tokyo 113-0033, Japan

(Received 7 May 2020; accepted 21 July 2021; published 13 August 2021)

It is highly nontrivial to what extent we can deduce the relaxation behavior of a quantum dissipative system from the spectral gap of the Liouvillian that governs the time evolution of the density matrix. We investigate the relaxation processes of a quantum dissipative system that exhibits the Liouvillian skin effect, which means that the eigenmodes of the Liouvillian are localized exponentially close to the boundary of the system, and find that the timescale for the system to reach a steady state depends not only on the Liouvillian gap Δ, but also on the localization length ξ of the eigenmodes. In particular, we show that the longest relaxation time τ that is maximized over initial states and local observables is given by $\tau \sim \Delta^{-1}(1 + L/\xi)$ with L being the system size. This implies that the longest relaxation time can diverge for $L \to \infty$ without gap closing.

DOI: 10.1103/PhysRevLett.127.070402

Introduction.—Relaxation processes of quantum systems coupled to environments are among the most fundamental nonequilibrium phenomena in condensed matter physics. Recent experimental advances in atomic, molecular, and optical (AMO) systems provide a highly controllable platform to study dissipative dynamics of various quantum systems [1–6]. A crucial question here is what determines the timescale for a given system to reach a steady state. This problem is of great relevance to applications, because controlling the relaxation time of a quantum system is a key to quantum control and information processing [7–12].

The spectral gap plays a crucial role in characterizing the relaxation time. In isolated quantum systems, the spectral gap of a Hamiltonian determines the timescale of low-energy excitations. The timescale diverges at a critical point where the spectral gap closes [13]. In quantum dissipative systems, the relaxation dynamics is characterized by the eigenspectrum and eigenmodes of a Liouvillian that governs the time evolution of the density matrix. The Liouvillian spectral gap (or the asymptotic decay rate) Δ is defined as the smallest modulus of the real part of nonzero eigenvalues. It has been postulated in many studies that the longest relaxation timescale of a quantum dissipative system is given by Δ^{-1} [14–16]. It is also known that in dissipative phase transitions the closing of the Liouvillian gap results in the divergence of the relaxation timescale [17–20]. However, while the Liouvillian gap characterizes asymptotic convergence to a steady state, transient behavior cannot generally be inferred from the gap alone. In fact, significant differences are known to arise between the spectral gap and the mixing time, which are called cutoff phenomena [21–25]. It is therefore natural to ask whether there is a general relationship that links transient relaxation behavior not only to the spectral gap, but also to other properties of the Liouvillian.

In this Letter, we present a general relationship among the relaxation time, the Liouvillian gap, and the spatial structure of Liouvillian eigenmodes for quantum dissipative systems in which some eigenmodes are exponentially localized near a boundary of the system. In dissipative systems driven out of equilibrium, localization phenomena of excitation modes near boundaries have attracted much attention in the context of the bulk-edge correspondence in non-Hermitian topological matter, known as the non-Hermitian skin effect [26–35]. Here, we refer to the localization of Liouvillian eigenmodes as the Liouvillian skin effect to emphasize that our study concerns Liouvillian spectra. We derive a relation between the maximal relaxation time, the Liouvillian gap, and the localization length of eigenmodes [see Eq. (8)]. We also propose a prototypical asymmetric-hopping model that exhibits the Liouvillian skin effect.

Liouvillian skin effect and relaxation time.—Within the Born-Markov approximation [36,37], the time evolution of the density matrix $\hat{\rho}$ is described by a master equation [38,39]:

$$\frac{d\hat{\rho}}{dt} = \mathcal{L}(\hat{\rho}) := -i[\hat{H}, \hat{\rho}] + \sum_{\alpha} \left(\hat{L}_{\alpha} \hat{\rho} \hat{L}_{\alpha}^{\dagger} - \frac{1}{2} \{ \hat{L}_{\alpha}^{\dagger} \hat{L}_{\alpha}, \hat{\rho} \} \right), \quad (1)$$

where $\hat{H}$ is the Hamiltonian of the system, $\hat{L}_\alpha$ is the Lindblad operator, $[\hat{A},\hat{B}] \equiv \hat{A}\hat{B} - \hat{B}\hat{A}$, and $\{\hat{A},\hat{B}\} \equiv \hat{A}\hat{B} + \hat{B}\hat{A}$. The Planck constant $\hbar$ is set to unity throughout this Letter. The Born-Markov approximation is known to be justified for typical AMO systems such as trapped two-level atoms with spontaneous emission and an optical cavity with photon loss [36,37]. We denote the dimension of the Hilbert space of the system as D. With the inner product $(\hat{A}|\hat{B}) := \mathrm{Tr}[\hat{A}^\dagger \hat{B}]$, a set of operators forms a D^2-dimensional Hilbert space. The right and left eigenmodes of the Liouvillian $\mathcal{L}$ are defined by

$$\mathcal{L}(\hat{\rho}_j^R) = \lambda_j \hat{\rho}_j^R, \qquad \mathcal{L}^\dagger(\hat{\rho}_j^L) = \lambda_j^* \hat{\rho}_j^L \quad (j = 0, 1, \ldots, D^2 - 1), \tag{2}$$

where λ_j is the jth eigenvalue and $\mathcal{L}^\dagger$ is given by

$$\mathcal{L}^\dagger(\hat{\rho}) = -i[\hat{\rho}, \hat{H}] + \sum_\alpha \left(\hat{L}_\alpha^\dagger \hat{\rho} \hat{L}_\alpha - \frac{1}{2}\{\hat{L}_\alpha^\dagger \hat{L}_\alpha, \hat{\rho}\} \right). \tag{3}$$

The steady state $\hat{\rho}_{\mathrm{ss}}$ is the right eigenmode corresponding to the zero eigenvalue, $\mathcal{L}(\hat{\rho}_{\mathrm{ss}}) = 0$, and we set $\hat{\rho}_0^R = \hat{\rho}_{\mathrm{ss}}$. Suppose that all eigenvalues are arranged in descending order of their real parts: $0 = \mathrm{Re}[\lambda_0] > \mathrm{Re}[\lambda_1] \geq \cdots \geq \mathrm{Re}[\lambda_{D^2-1}]$. Each eigenmode is normalized as $\|\hat{\rho}_j^R\|_{\mathrm{tr}} = \|\hat{\rho}_j^L\|_{\mathrm{tr}} = 1$, where $\|\hat{A}\|_{\mathrm{tr}} := \mathrm{Tr}[(\hat{A}^\dagger \hat{A})^{1/2}]$. The right and left eigenmodes corresponding to different eigenvalues are orthogonal to each other: $(\hat{\rho}_j^L|\hat{\rho}_k^R) = 0 (\lambda_j \neq \lambda_k)$.

An arbitrary initial state $\hat{\rho}_{\mathrm{ini}}$ can be expanded as

$$\hat{\rho}_{\mathrm{ini}} = \hat{\rho}_{\mathrm{ss}} + \sum_{j=1}^{D^2-1} c_j \hat{\rho}_j^R, \tag{4}$$

where c_j is written as

$$c_j = \frac{(\hat{\rho}_j^L|\hat{\rho}_{\mathrm{ini}})}{(\hat{\rho}_j^L|\hat{\rho}_j^R)}. \tag{5}$$

The time evolution of the density matrix is given by

$$\hat{\rho}(t) = \hat{\rho}_{\mathrm{ss}} + \sum_{j=1}^{D^2-1} c_j e^{\lambda_j t} \hat{\rho}_j^R. \tag{6}$$

The Liouvillian gap is defined by $\Delta = |\mathrm{Re}[\lambda_1]|$, which is also called the asymptotic decay rate [20].

We define the relaxation time of the system. The expectation value of a local observable $\hat{O}$ at time t and that for the steady state are denoted as $O(t) = \mathrm{Tr}[\hat{O}\hat{\rho}(t)]$ and $O_{\mathrm{ss}} = \mathrm{Tr}[\hat{O}\hat{\rho}_{\mathrm{ss}}]$, respectively. First, we define $\tilde{\tau}(\hat{\rho}_{\mathrm{ini}}, \hat{O})$ as the largest time t that satisfies $|O(t) - O_{\mathrm{ss}}| \geq e^{-1}|O(0) - O_{\mathrm{ss}}|$, where we assume that $O(0) \neq O_{\mathrm{ss}}$ to ensure the finiteness of $\tilde{\tau}$. We also define the maximal relaxation time τ by taking the supremum of $\tilde{\tau}(\hat{\rho}_{\mathrm{ini}}, \hat{O})$ over all $\hat{\rho}_{\mathrm{ini}}$ and $\hat{O}$ under the condition $O(0) \neq O_{\mathrm{ss}}$. If one takes the initial state $\hat{\rho}_{\mathrm{ini}} = \hat{\rho}_{\mathrm{ss}} + c_j \hat{\rho}_j^R + c_j^* (\hat{\rho}_j^R)^\dagger$ with arbitrary $j (\neq 0)$, the relaxation time is given by $\tilde{\tau}(\hat{\rho}_{\mathrm{ini}}, \hat{O}) = \mathrm{Re}[\lambda_j]^{-1}$. By maximizing $\tilde{\tau}$ over $\hat{\rho}_{\mathrm{ini}}$, it is natural to expect

$$\tau \overset{?}{=} \frac{1}{\Delta}. \tag{7}$$

If Eq. (7) were true, the necessary and sufficient condition for the divergence of the maximal relaxation time would be closing of the Liouvillian gap.

We show that Eq. (7) does not hold if the system exhibits the Liouvillian skin effect. For simplicity, we consider a single-particle system in a one-dimensional space of length L. Let $|x\rangle$ be the state in which the particle is located at position x. We assume that the matrix element of the first right (left) eigenmode is exponentially localized near the right (left) boundary: $|\langle x|\hat{\rho}_1^R|y\rangle| \sim e^{-(2L-x-y)/\xi}$ [$|\langle x|\hat{\rho}_1^L|y\rangle| \sim e^{-(x+y)/\xi}$], where ξ is the localization length. Then, the overlap between them is exponentially small: $(\hat{\rho}_1^L|\hat{\rho}_1^R) \sim e^{-O(L/\xi)}$. Note that the numerator of Eq. (5) is maximized and takes a value of $O(1)$ when $\hat{\rho}_{\mathrm{ini}}$ is localized near the left boundary. Thus, the maximal $|c_1|$ over all initial states is proportional to $e^{O(L/\xi)}$. It is reasonable to state that the system has reached a steady state if $|O(t) - O_{\mathrm{ss}}| \ll \|\hat{O}\|_{\mathrm{op}}$ for any local observable $\hat{O}$, where $\|\ldots\|_{\mathrm{op}}$ denotes the operator norm. From Eq. (6), we have $|\sum_{j>0} c_j e^{\lambda_j t} \mathrm{Tr}[\hat{O}\hat{\rho}_j^R]| \ll \|\hat{O}\|_{\mathrm{op}}$, where each $|\mathrm{Tr}[\hat{O}\hat{\rho}_j^R]|$ is bounded by $\|\hat{O}\|_{\mathrm{op}}$. Since in a later stage of relaxation the slowest mode ($j = 1$) is expected to be dominant in the sum of the left-hand side, the condition for the system to reach its steady state is given by $|c_1|e^{-t\Delta} \ll 1$. Thus, the maximal relaxation time τ is given by $|c_1|e^{-\tau\Delta} = e^{-1}$. From $|c_1| \sim e^{O(L/\xi)}$, we find

$$\tau \sim \frac{1}{\Delta} + \frac{L}{\xi\Delta}. \tag{8}$$

This is the main result of this Letter. In the absence of the skin effect, i.e., $\xi = L$, Eq. (8) reduces to Eq. (7). Equation (8) implies that, if the Liouvillian gap and the localization length are independent of the system size, the maximal relaxation time is proportional to the system size. Defining the relaxation velocity by $v_R := L/\tau$, Eq. (8) gives

$$v_R \sim \xi\Delta \tag{9}$$

for $L \to \infty$. It should be noted that the derivation of Eq. (8) does not rely on the details of the Liouvillian superoperator, as long as its eigenmodes exhibit the skin effect. While we

here focus on the Lindblad master equation, the same argument can also be applied to other types of master equations, such as the Redfield equation.

We here note the relationship between the relaxation time τ defined above and the mixing time in Markov processes [21–25]. The maximal distance to the steady state over initial states is given by $d(t) = \max_{\hat{\rho}_{\rm ini}} \|\hat{\rho}(t) - \hat{\rho}_{\rm ss}\|_{\rm tr}$. The mixing time $\tau_{\rm mix}$ is then defined as the time for $d(t)$ to reach some small value ϵ. In general, $\tau_{\rm mix}$ provides an upper bound on the relaxation time of observables. When $\hat{\rho}_{\rm ss}$ is localized, $\max_{\hat{\rho}_{\rm ini}} \tilde{\tau}(\hat{\rho}_{\rm ini}, \hat{O})$ attains $\tau_{\rm mix}$ for local observables $\hat{O}$ with support in the localized region of $\hat{\rho}_{\rm ss}$, and, thus, the maximal relaxation time τ over all local observables coincides with $\tau_{\rm mix}$. Therefore, Eq. (8) is also valid for the mixing time.

Prototypical model.—Here, we present a prototypical model that shows the Liouvillian skin effect. The Hamiltonian of the system is given by $\hat{H} = -J\sum_{l=1}^{L}(\hat{b}_{l+1}^{\dagger}\hat{b}_l + \hat{b}_l^{\dagger}\hat{b}_{l+1})$, where $\hat{b}_l^{\dagger}$ and $\hat{b}_l$ are the creation and annihilation operators, respectively, of a boson at site l, which satisfy $[\hat{b}_l, \hat{b}_m^{\dagger}] = \delta_{lm}$ and $[\hat{b}_l, \hat{b}_m] = [\hat{b}_l^{\dagger}, \hat{b}_m^{\dagger}] = 0$, and J represents the transfer amplitude. We consider Lindblad operators $\hat{L}_{R,l} = \sqrt{\gamma_R}\hat{b}_{l+1}^{\dagger}\hat{b}_l$ and $\hat{L}_{L,l} = \sqrt{\gamma_L}\hat{b}_{l-1}^{\dagger}\hat{b}_l$ [40,41], which describe stochastic hopping to the right and left neighboring sites with rates γ_R and γ_L, respectively. The index α in Eq. (1) includes R or L, and site index $l = 1, 2, \ldots, L$. We will discuss both cases of the open boundary condition (OBC) and the periodic boundary condition (PBC). Given the state $|l\rangle$ in which the particle is located at site l, the set of vectors $\{|l\rangle\}_{l=1,\ldots,L}$ forms an orthonormal basis of the Hilbert space. The asymmetric stochastic hopping can be implemented with ultracold atoms in an optical lattice by laser-assisted hopping with spontaneous emission [42–47]. While such an experimental setup also gives rise to an on-site dephasing $\hat{L}_{d,l} = \sqrt{\gamma_d}\hat{b}_l^{\dagger}\hat{b}_l$, this additional dissipation does not affect the qualitative behaviors discussed below [47].

Relaxation time.—Suppose that the initial state is localized at a point with distance d from the region in which the steady state is localized. Since the total particle number $\hat{N} = \sum_{l=1}^{L}\hat{b}_l^{\dagger}\hat{b}_l$ is conserved, the relaxation toward the steady state must be accompanied by the transport of particles. In quantum dissipative systems with local interactions, there exists an upper bound on the speed at which information can propagate, i.e., the Lieb-Robinson bound [52,53]. Thus, it takes a time at least proportional to d for the system to reach its steady state. In other words, the maximal relaxation time diverges in the limit of infinite system size.

Let us confirm this fact by numerically solving the master equation under the OBC. Figure 1(a) shows the time evolution of the density profile $n_l = \mathrm{Tr}[\hat{\rho}\hat{b}_l^{\dagger}\hat{b}_l] = \langle l|\hat{\rho}|l\rangle$ from an initial state $\hat{\rho}_{\rm ini} = |1\rangle\langle 1|$. For $\gamma_R > \gamma_L$, the particle

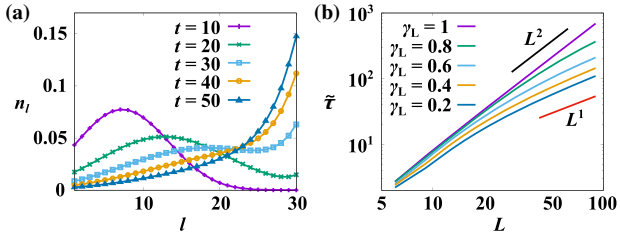

FIG. 1. (a) Time evolution of the density profile n_l with hopping parameters $J = \gamma_R = 1$ and $\gamma_L = 0.5$ and system size $L = 30$. (b) Relaxation time $\tilde{\tau}$ with hopping parameters $J = \gamma_R = 1$ and $\gamma_L = 1, 0.8, 0.6, 0.4, 0.2$ from top to bottom. The abscissa and ordinate are shown in log scales. The two straight lines represent the L^1 and L^2 scalings.

is transported from left to right and accumulated at the right boundary. Figure 1(b) shows $\tilde{\tau}$ determined from the condition $n_{{\rm ss},L} - n_L(\tilde{\tau}) = e^{-1}n_{{\rm ss},L}$, where $n_{{\rm ss},l}$ is the density profile of the steady state. For $\gamma_R = \gamma_L$, $\tilde{\tau}$ is proportional to L^2, reflecting the diffusive relaxation to the uniform steady state. In contrast, for $\gamma_R > \gamma_L$, $\tilde{\tau}$ is asymptotically proportional to L. If the relation (7) were correct, the gap should always close.

Liouvillian spectrum.—The operator space is spanned by $\{|l\rangle\langle m|\}_{l,m=1,\ldots,L}$. First, we consider the case of $J = 0$, where the action of $\mathcal{L}$ is closed in the diagonal subspace spanned by $\{|l\rangle\langle l|\}_{l=1,\ldots,L}$ and in the off-diagonal subspace spanned by $\{|l\rangle\langle m|\}_{l,m=1,\ldots,L;l\neq m}$ [47]. If we interpret $|l\rangle\langle l|$ as the state in which a particle sits at site l, then $\mathcal{L}$ restricted to the diagonal subspace is equivalent to a non-Hermitian tight-binding Hamiltonian

$$\hat{\mathcal{H}}_{\rm PBC} = \sum_{l=1}^{L}(\gamma_R\hat{c}_{l+1}^{\dagger}\hat{c}_l + \gamma_L\hat{c}_l^{\dagger}\hat{c}_{l+1}) \tag{10}$$

for the PBC and

$$\hat{\mathcal{H}}_{\rm OBC} = \sum_{l=1}^{L-1}(\gamma_R\hat{c}_{l+1}^{\dagger}\hat{c}_l + \gamma_L\hat{c}_l^{\dagger}\hat{c}_{l+1}) + \gamma_L\hat{c}_1^{\dagger}\hat{c}_1 + \gamma_R\hat{c}_L^{\dagger}\hat{c}_L \tag{11}$$

for the OBC, where $\hat{c}_l^{\dagger}$ and $\hat{c}_l$ are the creation and annihilation operators, respectively, of the virtual particle and we have omitted a constant energy shift $-\gamma_R - \gamma_L$. Such a tight-binding model with asymmetric hopping is known as the Hatano-Nelson model [27,54–56].

For the case of the PBC, a right eigenmode of $\hat{\mathcal{H}}_{\rm PBC}$ is given by a plane wave $\psi_{k,l} \propto e^{ikl}$ with $k = 2\pi n/L$ $(n = -L/2 + 1, \ldots, L/2)$, and its eigenvalue reads

$$\lambda_k^{\rm (PBC)} = \gamma_R e^{-ik} + \gamma_L e^{ik} - \gamma_R - \gamma_L, \tag{12}$$

where we have restored the constant shift $-\gamma_R-\gamma_L$. From Eq. (12), we have $\Delta\sim L^{-2}$.

Next, we consider the eigenmodes of $\hat{\mathcal{H}}_{\mathrm{OBC}}$. We introduce an imaginary gauge transformation $\hat{V}=\exp[-\ln r\sum_l l\hat{c}_l^\dagger\hat{c}_l]$, which gives $\hat{V}^{-1}\hat{c}_l^\dagger\hat{V}=r^l\hat{c}_l^\dagger$ and $\hat{V}^{-1}\hat{c}_l\hat{V}=r^{-l}\hat{c}_l$ [54–56]. When $r=\sqrt{\gamma_L/\gamma_R}$, the transformed Hamiltonian $\hat{\mathcal{H}}'_{\mathrm{OBC}}:=\hat{V}^{-1}\hat{\mathcal{H}}_{\mathrm{OBC}}\hat{V}$ is given by replacing γ_R and γ_L in the hopping term $\gamma_R\hat{c}_{l+1}^\dagger\hat{c}_l+\gamma_L\hat{c}_l^\dagger\hat{c}_{l+1}$ in Eq. (11) with $\sqrt{\gamma_R\gamma_L}$. Note that the eigenspectrum of $\hat{\mathcal{H}}_{\mathrm{OBC}}$ is real, because $\hat{\mathcal{H}}'_{\mathrm{OBC}}$ is Hermitian. Let ψ_l and ψ'_l be a right eigenmode of $\hat{\mathcal{H}}_{\mathrm{OBC}}$ and that of $\hat{\mathcal{H}}'_{\mathrm{OBC}}$ sharing the same eigenvalue. The right eigenmodes of $\hat{\mathcal{H}}'_{\mathrm{OBC}}$ include a bound state $\psi'_{\mathrm{BS},l}\propto(\gamma_R/\gamma_L)^{l/2}$ and $(L-1)$ plane-wave states $\psi'_{k,l}=c_1e^{ikl}+c_2e^{-ikl}$ with $k=n\pi/L$ $(n=1,\ldots,L-1)$ [47]. The bound state corresponds to the steady state. The eigenvalues for the plane-wave states are given by

$$\lambda_k^{(\mathrm{OBC})}=2\sqrt{\gamma_R\gamma_L}\cos k-\gamma_R-\gamma_L. \tag{13}$$

The eigenmode of the original Hamiltonian $\hat{\mathcal{H}}_{\mathrm{OBC}}$ is given by $\psi_l=(\gamma_R/\gamma_L)^{l/2}\psi'_l$. When $\gamma_R>\gamma_L$, all right eigenmodes are exponentially localized near the right boundary. From Eq. (13), the gap is given by

$$\Delta=\gamma_R+\gamma_L-2\sqrt{\gamma_R\gamma_L} \tag{14}$$

in the $L\to\infty$ limit. Note that, for $\gamma_R=\gamma_L$, the gap closes as L^{-2}. Thus, in sharp contrast to the case of the PBC, the Liouvillian spectrum under the OBC has a nonvanishing gap for $\gamma_R\neq\gamma_L$. Such an extreme sensitivity of the eigenspectrum to the boundary conditions is a special character of quantum dissipative systems driven out of equilibrium and reminiscent of a similar effect seen in the non-Hermitian systems [26–35]. The left eigenmodes of $\hat{\mathcal{H}}_{\mathrm{OBC}}$ can be obtained by exchanging γ_R and γ_L in the right eigenmodes. Thus, for $\gamma_R>\gamma_L$, the left eigenmodes are localized near the left boundary.

The eigenvalues given by Eqs. (12) and (13) are those of $\mathcal{L}$ that are restricted to the diagonal subspace. In addition to them, there are (L^2-L) eigenvalues belonging to the off-diagonal subspace. For the PBC, it is given by $\lambda=-\gamma_R-\gamma_L$. For the OBC, there are four eigenvalues $\lambda=-\gamma_R-\gamma_L$, $-\gamma_R-\gamma_L/2$, $-\gamma_R/2-\gamma_L$, and $-\gamma_R/2-\gamma_L/2$, whose degeneracies are $(L-2)(L-3)$, $2(L-2)$, $2(L-2)$, and 2, respectively.

For $J\neq0$, the eigenvalue problem of the Liouvillian cannot be solved exactly, and we study its eigenspectrum using numerical diagonalization. Figure 2 shows Δ as a function of L. For the PBC case (a), Δ vanishes as L^{-2} for arbitrary hopping parameters. For the OBC case (b), while $\Delta\sim L^{-2}$ for $\gamma_R=\gamma_L$, Δ approaches a nonzero value for $\gamma_R\neq\gamma_L$ [16].

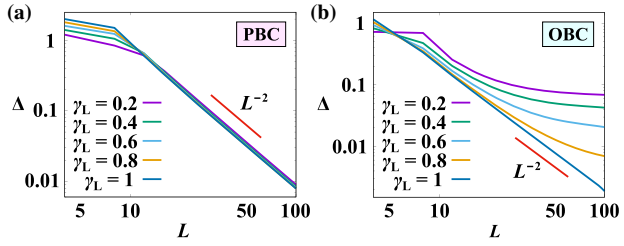

FIG. 2. Liouvillian gap Δ as a function of the system size L for the PBC (a) and the OBC (b) with $J=\gamma_R=1$ and $\gamma_L=0.2$, 0.4, 0.6, 0.8, and 1. The abscissa and ordinate are shown in log scales. The straight solid lines represent the L^{-2} scaling.

Next, we show that the eigenmodes exhibit the Liouvillian skin effect for nonzero J. Figures 3(a) and 3(b) show $\{\lambda_j\}_{j=0,\ldots,L^2-1}$ for the OBC. The eigenspectrum is composed of two groups of eigenvalues with and without imaginary parts. The real spectrum stems from the eigenvalues given by Eq. (13) at $J=0$. One can clearly see two clusters of complex eigenvalues around $\mathrm{Re}[\lambda]=-\gamma_R-\gamma_L=-1.2$ and $\mathrm{Re}[\lambda]=-\gamma_R/2-\gamma_L=-0.7$, which originate from the highly degenerated eigenvalues at $J=0$. Figure 3(c) shows the modulus of $\rho^R_{j,lm}=\langle l|\hat{\rho}^R_j|m\rangle$ for the eigenvalues indicated by arrows (i)–(iv) in Fig. 3(a). For the real eigenvalues such as (i) and (iv), $\rho^R_{j,lm}$ is localized exponentially near the right boundary. In contrast, for the complex eigenvalues such as (ii) and (iii), $\rho^R_{j,lm}$ is delocalized for one or both of l and m. The partial skin effect observed in (ii) can be understood from the fact that $\hat{\rho}^R_j$ is a superposition of $|l\rangle\langle m|$ where either l or m belongs to the right boundary, which is the eigenmode with $\lambda=-\gamma_R/2-\gamma_L$ at $J=0$. The eigenmodes with the complex eigenvalues are irrelevant to the slowing down of relaxation, because they do not exhibit the Liouvillian skin effect.

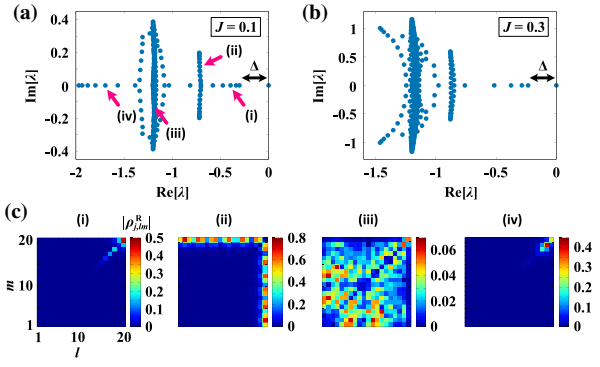

FIG. 3. (a), (b) Liouvillian eigenspectrum for the OBC with $\gamma_R=1$, $\gamma_L=0.2$, and $J=0.1$ (a) and $J=0.3$ (b). The system size is $L=20$. (c) Color plots of $|\rho^R_{j,lm}|$ corresponding to the eigenvalues indicated by arrows (i)–(iv) in (a).

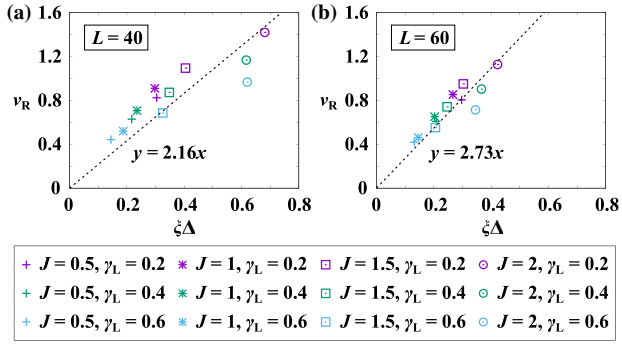

FIG. 4. Plots of v_R versus $\xi\Delta$ with $\gamma_R = 1$, and $J = 0.5$ (cross), 1 (star), 1.5 (square), and 2 (circle), and $\gamma_L = 0.2$ (purple), 0.4 (green), and 0.6 (blue). The system sizes are (a) $L = 40$ and (b) $L = 60$. The dashed lines represent the least squares fitting by $y = ax$. The relative standard error of a is 6.5% for (a) and 4.0% for (b).

Let us confirm Eq. (9) for the prototypical model. We assume that ξ is of the same order of magnitude as the localization length of the steady state. By using the density profile $n_{\mathrm{ss},l}$ of the steady state, ξ is estimated to be $\xi = 1/n_{\mathrm{ss},L}$. Figure 4 shows v_R and $\xi\Delta$ for several parameters. As the system size increases, the plots of v_R versus $\xi\Delta$ converge to points on a single line $v_R = a\xi\Delta$ with $a \simeq 2.7$.

To estimate the relaxation time in Figs. 1 and 4, we have focused on the diagonal elements $\rho_{ll} = \langle l|\hat{\rho}|l\rangle$ of the density matrix. It is also intriguing to consider the relaxation of the off-diagonal elements $\rho_{lm} = \langle l|\hat{\rho}|m\rangle (l \neq m)$, because they provide a measure of quantum coherence. For $J = 0$, since $\hat{\rho}_1^R$ does not contain the off-diagonal elements, ρ_{lm} decays at a constant rate and Eq. (8) does not hold. In contrast, for $J \neq 0$, the relaxation time of ρ_{lm} diverges with the system size [47], since the eigenmodes exhibiting the skin effect have nonzero off-diagonal elements [see (i) in Fig. 3].

Generalizations.—The prototypical model can be generalized to an N ($< L$)-particle system with the hard-core condition $(\hat{b}_l^\dagger)^2 = 0$. For $J = 0$, the model is identical to a classical Markov process known as the asymmetric simple exclusion process (ASEP) [57]. For the OBC, it has been proven that the transition matrix of the ASEP has a nonzero spectral gap in the thermodynamic limit [58]. The density profile n_l of the steady state is given by $n_{L-N-l} \propto e^{-l/\xi}$ and $n_{L-N+l} \propto 1 - e^{-l/\xi}$ when $\gamma_R > \gamma_L$. The existence of such an exponential tail in the density profile suggests that the overlap between the right and left eigenmodes should be exponentially small. Thus, Eq. (8) should hold for $J = 0$. It merits further study to investigate the validity of Eq. (8) for the many-body case with nonzero J.

The non-Hermitian skin effects in higher-dimensional systems are currently under active investigation [33–35]. Our results can also be extended to higher-dimensional cases. For example, a possible manifestation of the skin effect in a rectangular-shaped two-dimensional system is the localization of the right eigenmodes at one of the four edges of the boundary. If the left eigenmodes are localized at the opposite side, Eq. (8) holds by replacing the one-dimensional system size L by the length perpendicular to the edges at which the eigenmodes are localized. Understanding what factors determine the location of the eigenmode localization in higher-dimensional systems merits further study.

Finally, we remark on the non-Markovian effect in the dynamics of open quantum systems. As in the Markovian cases, one can also perform the spectral decomposition of the propagator corresponding to the temporally nonlocal master equation [59]. A major difference from the Markovian case is that the eigenmodes and the spectrum explicitly depend on time. If these time-dependent eigenmodes are always localized near the boundary, we can expect the slowing down of relaxation processes without gap closing.

Conclusions.—We have shown that the longest relaxation time of a quantum dissipative system depends not only on the Liouvillian gap, but also on the localization length of the eigenmodes. This behavior is a nonequilibrium effect unique to dissipative systems driven far from thermal equilibrium. In fact, it can be shown that, if the Liouvillian with a spatially uniform Hamiltonian satisfies the detailed balance condition, the right and left eigenmodes cannot be localized near opposite boundaries of the system [47]. It is worthwhile to study other mechanisms that lead to a small overlap between the right and left eigenmodes [22–25,60].

The authors thank T. Mori for helpful discussions. This work was supported by KAKENHI Grants No. JP19J00525 and No. JP18H01145 and a Grant-in-Aid for Scientific Research on Innovative Areas (KAKENHI Grant No. JP15H05855) from Japan Society for the Promotion of Science (JSPS). M. N. was supported by KAKENHI Grant No. JP20K14383. R. H. was supported by JSPS through Program for Leading Graduate Schools (ALPS) and JSPS fellowship (KAKENHI Grant No. JP17J03189).

*haga@pe.osakafu-u.ac.jp

[1] I. Bloch, Quantum coherence and entanglement with ultracold atoms in optical lattices, Nature (London) **453**, 1016 (2008).

[2] S. Diehl, A. Micheli, A. Kantian, B. Kraus, H. P. Büchler, and P. Zoller, Quantum states and phases in driven open quantum systems with cold atoms, Nat. Phys. **4**, 878 (2008).

[3] H. Weimer, R. Löw, T. Pfau, and H. P. Büchler, Quantum Critical Behavior in Strongly Interacting Rydberg Gases, Phys. Rev. Lett. **101**, 250601 (2008).

[4] A. Tomadin, S. Diehl, and P. Zoller, Nonequilibrium phase diagram of a driven and dissipative many-body system, Phys. Rev. A **83**, 013611 (2011).

[5] T. E. Lee, H. Häffner, and M. C. Cross, Antiferromagnetic phase transition in a nonequilibrium lattice of Rydberg atoms, Phys. Rev. A **84**, 031402(R) (2011).

[6] M. Ludwig and F. Marquardt, Quantum Many-Body Dynamics in Optomechanical Arrays, Phys. Rev. Lett. **111**, 073603 (2013).

[7] T. Pellizzari, S. A. Gardiner, J. I. Cirac, and P. Zoller, Decoherence, Continuous Observation, and Quantum Computing: A Cavity QED Model, Phys. Rev. Lett. **75**, 3788 (1995).

[8] D. Jaksch, J. I. Cirac, P. Zoller, S. L. Rolston, R. Côté, and M. D. Lukin, Fast Quantum Gates for Neutral Atoms, Phys. Rev. Lett. **85**, 2208 (2000).

[9] G. Balasubramanian, P. Neumann, D. Twitchen, M. Markham, R. Kolesov, N. Mizuochi, J. Isoya, J. Achard, J. Beck, J. Tissler, V. Jacques, P. R. Hemmer, F. Jelezko, and J. Wrachtrup, Ultralong spin coherence time in isotopically engineered diamond, Nat. Mater. **8**, 383 (2009).

[10] L. Isenhower, E. Urban, X. L. Zhang, A. T. Gill, T. Henage, T. A. Johnson, T. G. Walker, and M. Saffman, Demonstration of a Neutral Atom Controlled-NOT Quantum Gate, Phys. Rev. Lett. **104**, 010503 (2010).

[11] H. Weimer, M. Müller, I. Lesanovsky, P. Zoller, and H. P. Büchler, A Rydberg quantum simulator, Nat. Phys. **6**, 382 (2010).

[12] B. P. Lanyon, C. Hempel, D. Nigg, M. Müller, R. Gerritsma, F. Zähringer, P. Schindler, J. T. Barreiro, M. Rambach, G. Kirchmair, M. Hennrich, P. Zoller, R. Blatt, and C. F. Roos, Universal digital quantum simulation with trapped ions, Science **334**, 57 (2011).

[13] S. Sachdev, *Quantum Phase Transitions* (Cambridge University Press, Cambridge, England, 2001).

[14] Z. Cai and T. Barthel, Algebraic Versus Exponential Decoherence in Dissipative Many-Particle Systems, Phys. Rev. Lett. **111**, 150403 (2013).

[15] L. Bonnes, D. Charrier, and A. M. Läuchli, Dynamical and steady-state properties of a Bose-Hubbard chain with bond dissipation: A study based on matrix product operators, Phys. Rev. A **90**, 033612 (2014).

[16] M. Žnidarič, Relaxation times of dissipative many-body quantum systems, Phys. Rev. E **92**, 042143 (2015).

[17] E. M. Kessler, G. Giedke, A. Imamoglu, S. F. Yelin, M. D. Lukin, and J. I. Cirac, Dissipative phase transition in a central spin system, Phys. Rev. A **86**, 012116 (2012).

[18] M. Höning, M. Moos, and M. Fleischhauer, Critical exponents of steady-state phase transitions in fermionic lattice models, Phys. Rev. A **86**, 013606 (2012).

[19] B. Horstmann, J. I. Cirac, and G. Giedke, Noise-driven dynamics and phase transitions in fermionic systems, Phys. Rev. A **87**, 012108 (2013).

[20] F. Minganti, A. Biella, N. Bartolo, and C. Ciuti, Spectral theory of Liouvillians for dissipative phase transitions, Phys. Rev. A **98**, 042118 (2018).

[21] D. A. Levin, Y. Peres, and E. L. Wilmer, *Markov Chains and Mixing Times* (American Mathematical Society, Providence, 2008).

[22] P. Diaconis, The cutoff phenomenon in finite Markov chains, Proc. Natl. Acad. Sci. U.S.A. **93**, 1659 (1996).

[23] M. J. Kastoryano, D. Reeb, and M. M. Wolf, A cutoff phenomenon for quantum Markov chains, J. Phys. A **45**, 075307 (2012).

[24] M. J. Kastoryano and J. Eisert, Rapid mixing implies exponential decay of correlations, J. Math. Phys. (N.Y.) **54**, 102201 (2013).

[25] E. Vernier, Mixing times and cutoffs in open quadratic fermionic systems, SciPost Phys. **9**, 049 (2020).

[26] T. E. Lee, Anomalous Edge State in a Non-Hermitian Lattice, Phys. Rev. Lett. **116**, 133903 (2016).

[27] Z. Gong, Y. Ashida, K. Kawabata, K. Takasan, S. Higashikawa, and M. Ueda, Topological Phases of Non-Hermitian Systems, Phys. Rev. X **8**, 031079 (2018).

[28] S. Yao and Z. Wang, Edge States and Topological Invariants of Non-Hermitian Systems, Phys. Rev. Lett. **121**, 086803 (2018).

[29] F. K. Kunst, E. Edvardsson, J. C. Budich, and E. J. Bergholtz, Biorthogonal Bulk-Boundary Correspondence in Non-Hermitian Systems, Phys. Rev. Lett. **121**, 026808 (2018).

[30] C. H. Lee and R. Thomale, Anatomy of skin modes and topology in non-Hermitian systems, Phys. Rev. B **99**, 201103(R) (2019).

[31] F. Song, S. Yao, and Z. Wang, Non-Hermitian Skin Effect and Chiral Damping in Open Quantum Systems, Phys. Rev. Lett. **123**, 170401 (2019).

[32] D. S. Borgnia, A. J. Kruchkov, and R.-J. Slager, Non-Hermitian Boundary Modes and Topology, Phys. Rev. Lett. **124**, 056802 (2020).

[33] N. Okuma, K. Kawabata, K. Shiozaki, and M. Sato, Topological Origin of Non-Hermitian Skin Effects, Phys. Rev. Lett. **124**, 086801 (2020).

[34] R. Okugawa, R. Takahashi, and K. Yokomizo, Second-order topological non-Hermitian skin effects, Phys. Rev. B **102**, 241202(R) (2020).

[35] K. Kawabata, M. Sato, and K. Shiozaki, Higher-order non-Hermitian skin effect, Phys. Rev. B **102**, 205118 (2020).

[36] A. J. Daley, Quantum trajectories and open many-body quantum systems, Adv. Phys. **63**, 77 (2014).

[37] L. M. Sieberer, M. Buchhold, and S. Diehl, Keldysh field theory for driven open quantum systems, Rep. Prog. Phys. **79**, 096001 (2016).

[38] G. Lindblad, On the generators of quantum dynamical semigroups, Commun. Math. Phys. **48**, 119 (1976).

[39] V. Gorini, A. Kossakowski, and E. C. G. Sudarshan, Completely positive dynamical semigroups of *N*-level systems, J. Math. Phys. (N.Y.) **17**, 821 (1976).

[40] V. Eisler, Crossover between ballistic and diffusive transport: The quantum exclusion process, J. Stat. Mech. (2011) P06007.

[41] K. Temme, M. M. Wolf, and F. Verstraete, Stochastic exclusion processes versus coherent transport, New J. Phys. **14**, 075004 (2012).

[42] D. Jaksch and P. Zoller, Creation of effective magnetic fields in optical lattices: The Hofstadter butterfly for cold neutral atoms, New J. Phys. **5**, 56 (2003).

[43] M. Aidelsburger, M. Atala, M. Lohse, J. T. Barreiro, B. Paredes, and I. Bloch, Realization of the Hofstadter

Hamiltonian with Ultracold Atoms in Optical Lattices, Phys. Rev. Lett. **111**, 185301 (2013).

[44] H. Miyake, G. A. Siviloglou, C. J. Kennedy, W. C. Burton, and W. Ketterle, Realizing the Harper Hamiltonian with Laser-Assisted Tunneling in Optical Lattices, Phys. Rev. Lett. **111**, 185302 (2013).

[45] J. Dalibard and C. Cohen-Tannoudji, Atomic motion in laser light: Connection between semiclassical and quantum descriptions, J. Phys. B **18**, 1661 (1985).

[46] H. Pichler, A. J. Daley, and P. Zoller, Nonequilibrium dynamics of bosonic atoms in optical lattices: Decoherence of many-body states due to spontaneous emission, Phys. Rev. A **82**, 063605 (2010).

[47] See Supplemental Material at http://link.aps.org/supplemental/10.1103/PhysRevLett.127.070402 for details of the eigenvalue problem of the prototypical model, the relaxation dynamics of the off-diagonal elements of the density matrix, the physical implementation of the model, the effect of on-site dephasing on the Liouvillian skin effect, and the proof of the absence of the skin effect under the detailed balance condition, which includes Refs. [48–51].

[48] R. Chetrite and K. Mallick, Quantum fluctuation relations for the Lindblad master equation, J. Stat. Phys. **148**, 480 (2012).

[49] E. B. Davies, *Quantum Theory of Open Systems* (Institute of Mathematics and its Applications, London, 1979).

[50] H. Spohn and J. L. Lebowitz, Irreversible thermodynamics for quantum systems weakly coupled to thermal reservoirs, Adv. Chem. Phys. **38**, 109 (1978).

[51] K. Kawabata, K. Shiozaki, M. Ueda, and M. Sato, Symmetry and Topology in Non-Hermitian Physics, Phys. Rev. X **9**, 041015 (2019).

[52] E. Lieb and D. Robinson, The finite group velocity of quantum spin systems, Commun. Math. Phys. **28**, 251 (1972).

[53] D. Poulin, Lieb-Robinson Bound and Locality for General Markovian Quantum Dynamics, Phys. Rev. Lett. **104**, 190401 (2010).

[54] N. Hatano and D. R. Nelson, Localization Transitions in Non-Hermitian Quantum Mechanics, Phys. Rev. Lett. **77**, 570 (1996).

[55] N. Hatano and D. R. Nelson, Vortex pinning and non-hermitian quantum mechanics, Phys. Rev. B **56**, 8651 (1997).

[56] N. Hatano and D. R. Nelson, Non-hermitian delocalization and eigenfunctions, Phys. Rev. B **58**, 8384 (1998).

[57] B. Derrida, An exactly soluble non-equilibrium system: The asymmetric simple exclusion process, Phys. Rep. **301**, 65 (1998).

[58] S. Sandow and G. Schütz, On $U_q[SU(2)]$-symmetric driven diffusion, Europhys. Lett. **26**, 7 (1994).

[59] D. Chruściński and A. Kossakowski, Non-Markovian Quantum Dynamics: Local Versus Nonlocal, Phys. Rev. Lett. **104**, 070406 (2010).

[60] T. Mori and T. Shirai, Resolving a Discrepancy Between Liouvillian Gap and Relaxation Time in Boundary-Dissipated Quantum Many-Body Systems, Phys. Rev. Lett. **125**, 230604 (2020).